

Evidence for quasifission in the sub-barrier reaction of $^{30}\text{Si} + ^{238}\text{U}$ K. Nishio,¹ H. Ikezoe,¹ I. Nishinaka,¹ S. Mitsuoka,¹ K. Hirose,² T. Ohtsuki,² Y. Watanabe,³
Y. Aritomo,^{1,4} and S. Hofmann^{5,6}¹*Japan Atomic Energy Agency, Tokai, Ibaraki 319-1195, Japan*²*Laboratory of Nuclear Science, Tohoku University, Sendai 982-0826, Japan*³*High Energy Accelerator Research Organization (KEK), Tsukuba, Ibaraki 305-0801, Japan*⁴*Flerov Laboratory of Nuclear Reactions, 141 980 Dubna, Russia*⁵*GSI Helmholtzzentrum für Schwerionenforschung, D-64291 Darmstadt, Germany*⁶*Institut für Kernphysik, Goethe-Universität Frankfurt, D-60438 Frankfurt am Main, Germany*

(Received 13 June 2010; published 7 October 2010)

Fragment mass distributions for fission after full momentum transfer were measured for the $^{30}\text{Si} + ^{238}\text{U}$ reaction at bombarding energies around the Coulomb barrier. At energies above the Bass barrier, the mass distributions were Gaussian with mass symmetry. An asymmetric fission channel with mass $A_L/A_H \approx 90/178$ emerged at the sub-barrier energies, where competition between fusion and quasifission was suggested from the evaporation residue (ER) cross section produced in the fusion $^{30}\text{Si} + ^{238}\text{U}$. We thus conclude the asymmetric channel is attributed to quasifission. It was supported by a model calculation using the Langevin equation to give the fragment mass distribution, where fusion-fission and quasifission were separated. The observed mass asymmetry for quasifission as well as the calculation is significantly smaller than those observed in actinide targets bombarded with heavier projectiles, which suggests that the system $^{30}\text{Si} + ^{238}\text{U}$ approaches the shape of the compound nucleus before disintegrating as quasifission.

DOI: [10.1103/PhysRevC.82.044604](https://doi.org/10.1103/PhysRevC.82.044604)

PACS number(s): 25.70.Jj, 25.60.Pj, 25.85.Ge

I. INTRODUCTION

Experimental challenges to produce superheavy nuclei (SHN) have been carried out by using heavy ion fusion reactions [1–3]. Development of a theoretical model to predict cross sections for nuclei located at the extreme end of heavy elements is important for the proper selection of target and projectile as well as the bombarding energy. The reaction is considered to proceed in three steps: (1) penetration of the Coulomb barrier between two colliding nuclei, (2) formation of a compound nucleus after the system is captured inside the Coulomb barrier, and (3) survival of the excited compound nucleus against fission (fusion-fission) to produce evaporation residue (ER).

The first step, penetrating the Coulomb barrier, is relatively well understood. The enhancement of the capture cross section (σ_{cap}) relative to the one-dimensional barrier penetration model was observed at the sub-barrier energy, which is explained by the distribution of the Coulomb barrier, as a result of coupling the incident flux to the collective states in the interacting nuclei. Deformation of the target and projectile is another reason for enhancing the capture cross sections. The second process, forming a compound nucleus (fusion probability), is not well understood. The theoretical model must treat the dynamic evolution of a system from the initial touching configuration up to the so-called compound nucleus state. In a reaction using a heavy target and projectile, which is the case for the production of the heaviest element, quasifission competes against fusion. Once the fusion cross section is calculated, it is multiplied by the survival probability, which can be determined by a statistical model, to calculate the cross section of SHN.

Measurement of the ER cross sections gives information on the fusion probability. However, because of the low production

rate for SHN, available data with high statistical accuracy are limited. When a model can treat fusion-fission and quasifission in a consistent framework, such as the unified theory [4], the measurement of fission properties can be another benchmark for testing the model, as fusion-fission and quasifission would have different decay properties.

Attempts to measure the fission properties in the heavy-ion collisions have been done for reactions leading to SHN [5–7] and also for reactions leading to lighter isotopes [8,9]. These measurements show that quasifission has the feature of asymmetric mass division. For the system $^{48}\text{Ca} + ^{168}\text{Er}$ leading to the lighter compound nucleus $^{216}\text{Ra}^*$, a pronounced suppression in the cross sections of ER was observed [10], which indicated the occurrence of quasifission. The mass distribution in this reaction [9] showed an asymmetric fission channel, whereas the more asymmetric reaction $^{12}\text{C} + ^{204}\text{Pb}$ leading to the same compound nucleus shows no asymmetric fission channel.

A strong variation in the mass distribution with energy was observed in the $^{36}\text{S} + ^{238}\text{U}$ [11] reaction. A symmetric mass distribution was observed in the higher energy region, where the projectile can collide on the equatorial side of the deformed nucleus ^{238}U with a prolate shape. In the sub-barrier energy, the distribution became asymmetric with peaks at $A_L/A_H \approx 74/200$. An increase in asymmetric fission probability with decreasing energy was interpreted as the enhanced quasifission probability, which was caused when the projectile collides on the polar sides of ^{238}U .

In this article, we report on the measurement of fission fragment mass distributions for $^{30}\text{Si} + ^{238}\text{U}$. In this reaction, the isotopes, ^{263}Sg and ^{264}Sg , were produced at above-barrier and sub-barrier energies, respectively, in the fusion-evaporation reaction [12]. From the cross section of ^{263}Sg

and the comparison with the statistical model calculation, no significant suppression for fusion was implied at the above-barrier energy, whereas the lower cross section for ^{264}Sg than the calculation suggested the appearance of quasifission at the sub-barrier energy. We expect to observe an asymmetric fission channel only at the sub-barrier energy. In this case a consistent picture on the appearance of quasifission and the drop of the ER cross section would be obtained in the SHN system for the first time. We will also discuss the mass asymmetry in the quasifission channel with those obtained for reactions using heavier projectiles and actinide targets.

II. EXPERIMENTAL DETAILS

The experiment was carried out using the ^{30}Si beams supplied from the JAEA tandem accelerator. The experimental setup and the analysis method are the same as described in Ref. [11]. Beam energies were changed around the Coulomb barrier energy to measure the energy dependence of fragment mass distributions as well as fission cross sections. Typical beam intensities were about 0.5–1.0 *particle-nA*. The ^{238}U target was prepared by an electrodeposition of natural UO_2 on Ni substrate 90 $\mu\text{g}/\text{cm}^2$ thick. The thickness of the ^{238}U was 80 $\mu\text{g}/\text{cm}^2$.

Both fission fragments (FFs) were detected in coincidence using position-sensitive multiwire proportional counters (MWPCs). The MWPCs have an active area of 200 mm horizontal by 120 mm vertical. The detectors were located on both sides of the target with a distance of 211 mm at angles of -61.0° for MWPC1 and $+90.0^\circ$ for MWPC2 with respect to the beam direction (see Fig. 1). Each MWPC covers the emission angles $\pm 25.0^\circ$ around the detector center. The detectors were operated with isobutane gas at a pressure of 3 Torr.

The time difference, ΔT , between the signals from two MWPCs was recorded. The time resolution of ΔT was $\sigma = 0.83$ ns (FWHM = 1.9 ns). The signals from both MWPCs contain information on the energy deposition, ΔE_1 and ΔE_2 , of particles passing through the detectors. From the fragment incident position on the MWPC, the emission angle for each fragment was determined. In the analysis, we separated fission events where the momentum of the projectile was fully transferred to the composite system [full momentum transfer (FMT)] by constructing the folding angle $\theta_{\text{fold}} = \theta_1 + \theta_2$ and the sum of out-of-plane angles $\phi_{\text{sum}} = \phi_1 + \phi_2$ (see Fig. 1), from the fission fragments from nuclei around ^{238}U produced by nucleon transfer reactions (see the following).

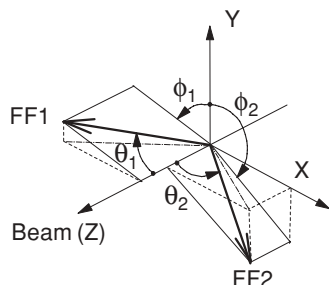


FIG. 1. Definition of the angles for fission fragment directions.

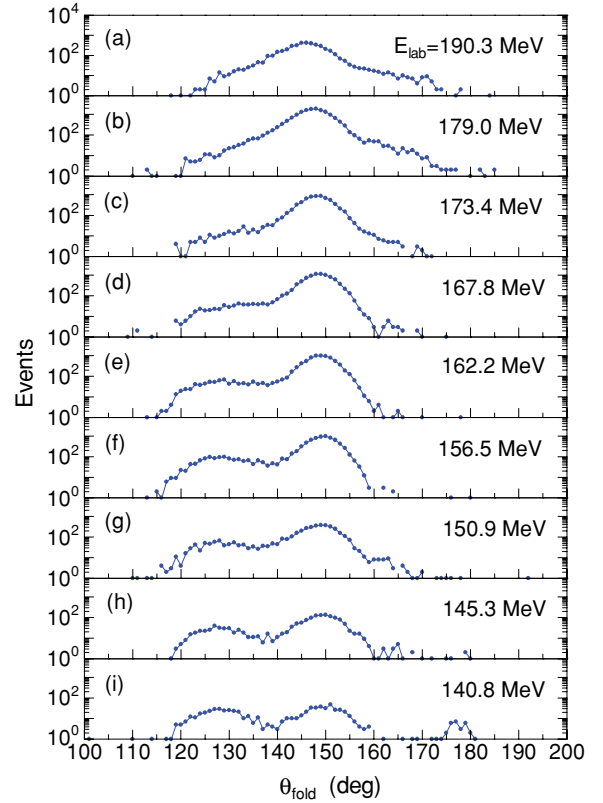


FIG. 2. (Color online) Distribution for folding angle of fission fragments produced in the $^{30}\text{Si} + ^{238}\text{U}$ reaction. The beam energy in the laboratory frame at the middle of the target is indicated.

III. EXPERIMENTAL RESULTS AND DISCUSSIONS

In the analysis, we constructed a two-dimensional spectrum of $(\Delta T, \Delta E_1 + \Delta E_2)$ as in Ref. [11] to separate the two coinciding fission events from the elastic-recoil events. From the fission events, we draw spectra for the folding angle θ_{fold} as shown in Fig. 2.

The FMT fissions are located around $\theta_{\text{fold}} = 146^\circ$ at the highest reaction energy $E_{\text{lab}} = 190.3$ MeV and around $\theta_{\text{fold}} = 150^\circ$ at the lowest energy 140.8 MeV. Fission following nucleon transfer has the larger folding angle than the FMT fission in the high-energy region above $E_{\text{lab}} = 179.0$ MeV, as seen in the tail of the spectrum larger than $\theta_{\text{fold}} = 160^\circ$. Below the energy of $E_{\text{lab}} = 173.4$ MeV, nucleon transfer fission is observed with a smaller folding angle than the FMT fission. These trends are explained by the angular dependence of the transfer reactions. Transfer reactions preferentially occur at the grazing angles (θ_{grazing}). The grazing angles are 83.4° at $E_{\text{lab}} = 190.3$ MeV and 141.1° at 162.2 MeV. For the former energy, the targetlike nuclei produced by transfer reaction will have smaller recoil energy in the beam direction than for FMT fission, resulting in a larger θ_{fold} value. For the latter energy, nucleon transfer fission has a smaller θ_{fold} value because of the larger recoil velocity. The FMT fission fragments were separated from the nuclear transfer fission on the $(\theta_{\text{fold}}, \phi_{\text{sum}})$ plane. In the higher energy region, the transfer fission events overlaps with the FMT fission and are not completely rejected. The yield for transfer-fission events entering in the analysis,

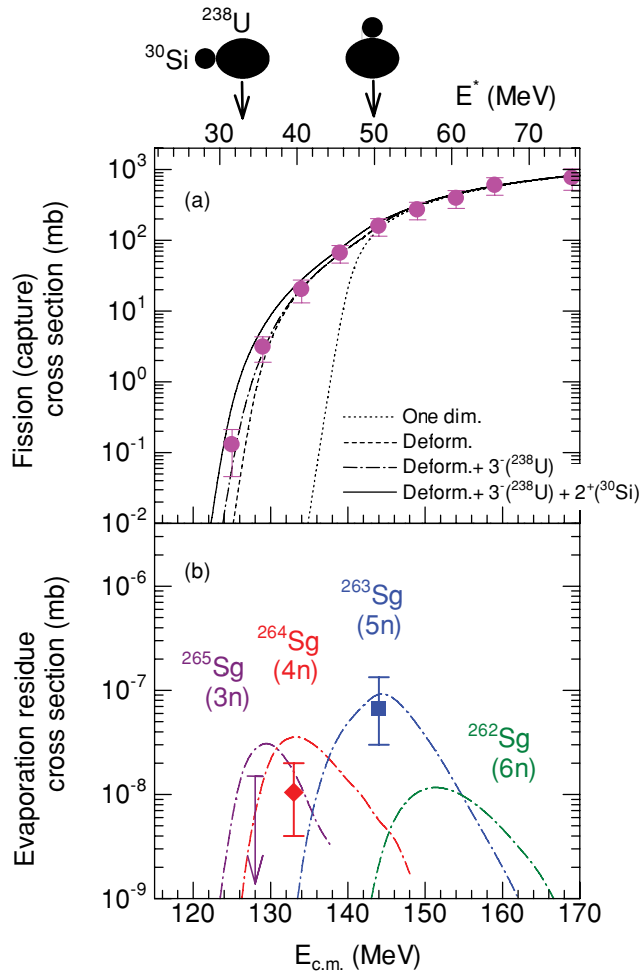


FIG. 3. (Color online) (a) Cross sections for the full momentum transfer (FMT) fission of the reactions $^{30}\text{Si} + ^{238}\text{U}$. The curves are the results of the calculations. The Coulomb barriers for polar and equatorial collisions are indicated. (b) Evaporation residue cross sections [12]. The curves are the results of statistical model calculation.

however, is less than 9%. At the sub-barrier energy region, the contamination is negligible.

The cross sections for the FMT fissions (σ_{fiss}) of $^{30}\text{Si} + ^{238}\text{U}$ are shown in Fig. 3(a) as a function of the center-of-mass energy $E_{c.m.}$. The cross section was obtained by fitting the fragment angular distribution in the center-of-mass angle of $85^\circ \leq \theta_{c.m.} \leq 125^\circ$ to a function described in Ref. [13] and integrating it over the solid angle. Because the angular range covered in the present experiment was limited, σ_{fiss} values contain an error arising from the uncertainties in $d\sigma_{\text{fiss}}/d\Omega(\theta_{c.m.})$ at forward and backward angles. We estimated a 28% uncertainty in σ_{fiss} in addition to the statistical uncertainty. The cross sections are almost equal to the capture cross sections (σ_{cap}).

The fission cross sections measured in Ref. [12] give larger values than the present result when they are compared at the lowest energy $E_{c.m.} = 125$ MeV. Our old data were determined by detecting a single fission fragment and thus we could not subtract fragments produced by nucleon transfer. As seen in Fig. 2, the yield for nucleon transfer fission relative to FMT

fission increases toward the low incident energy, so that the difference in the fission cross section between the coincidence and the single measurement increases at the deep sub-barrier energy.

In the inverse-kinematic experiment using ^{238}U beams and several target nuclei, the property of fission fragments were measured around the Coulomb barrier [5]. However, spectra for FMT fission and nucleon transfer fission were not reported.

To see the effects of nuclear properties on the capture cross sections, we show in Fig. 3 the calculation using the coupled-channels code, CCDEGEN [14], with several assumptions. The dotted curve is the result without considering any collective properties or deformation of the target and projectile (one-dimensional barrier penetration model). The calculation reproduces the data above the Coulomb barrier 139.7 MeV, but it decreases sharply below the barrier and cannot reproduce the data. The dashed curve is the result that takes into account the prolate deformation of ^{238}U with $(\beta_2, \beta_4) = (0.275, 0.050)$ [15]. The calculation reproduces within the error the experimental data down to $E_{c.m.} = 129.0$ MeV. The dash-dotted curve is the result additionally taking into account the coupling to the 3^- state at 0.73 MeV in ^{238}U ($\beta_3 = 0.086$ [16]). The calculation reproduces the data at the lowest incident energy $E_{c.m.} = 125.0$ MeV. The solid curve is obtained when the coupling to the 2^+ state at 2.235 MeV ($\beta_2 = 0.316$ [17]) in ^{30}Si is also considered. But the calculation overestimates the data at $E_{c.m.} = 129.0$ and 125.0 MeV. Coulomb barriers for the polar and equatorial collisions are 126.4 MeV to 143.4 MeV, respectively, and they are marked in the upper part of Fig. 3. The low Coulomb barrier for polar collisions is the main reason for the enhancement of the capture cross section at the sub-barrier energies.

Figure 4 shows the fragment mass distributions for the FMT fissions. The fragment masses were determined by applying the conservation law for momentum and mass with the assumption that mass of the composite system is equal to the sum of the projectile and target masses. The mass resolution was determined to be $\sigma = 2.7$ u (FWHM = 6.3 u) from the elastic scattering events. The mass distribution is scaled with the cross section such that the total cross section integrated over the mass gives twice the fission cross section shown in Fig. 3(a). To draw Fig. 4, we assumed that the mass distributions do not depend on $\theta_{c.m.}$. The distributions are Gaussian with symmetry in the energy range from $E_{c.m.} = 139.0$ MeV to 169.0 MeV. Changes to the spectrum appear at the sub-barrier energies of $E_{c.m.} = 134.0$ and 129.0 MeV, where the distribution has asymmetric component peaked at around $A_L/A_H \approx 90/178$. The sharp change can be characterized by the standard deviation of the mass distribution σ_m shown in Fig. 4. The value changes from $\sigma_m = 28.1 \pm 1.0$ u (139.0 MeV) to 37.5 ± 1.0 u (134.0 MeV). The difference in σ_m is far larger than the experimental mass resolution ($\sigma = 2.7$ u). The distribution at 129.0 MeV has a triple humped structure because of the enhanced asymmetric fission probability.

The asymmetric fission channel emerging at the sub-barrier energy apparently shows the different fission source. We conclude from the following argument that the asymmetric fission originates from quasifission. In Fig. 3(b), the measured ER cross sections [12] in this reaction are compared with a

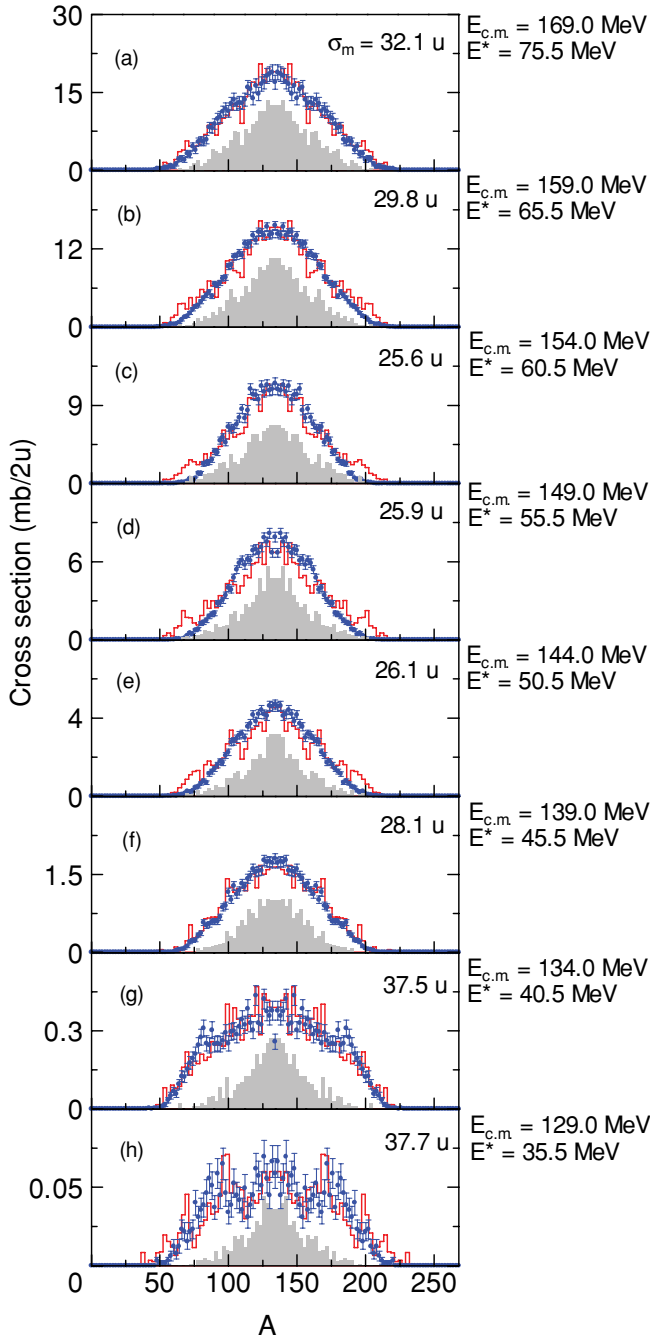


FIG. 4. (Color online) Fragment mass distributions for FMT fissions of the reaction $^{30}\text{Si} + ^{238}\text{U}$ (circle). The histogram shows a model calculation for FMT fissions using the Langevin equation. The calculated fusion-fission spectrum is shown by the filled area. Reaction energies in $E_{c.m.}$ and the excitation energy E^* for the compound nucleus are given. Standard deviation σ_m of the measured spectrum is shown. The error in σ_m is ± 1 u.

statistical model calculation under the assumption that the capture cross section, σ_{cap} , is equal to the fusion cross section. We used the dash-dotted curve as the fusion cross section in Fig. 3(a) (deformation of $^{238}\text{U} + 3^-$ state in ^{238}U), as it reproduces the fission cross sections at all the energy points. The partial cross sections at each energy $\sigma(L; E_{c.m.})$ were

determined by the CCDEGEN code and was input to the statistical model code HIVAP [18] to calculate the ER cross section.

The cross section for ^{263}Sg (5n) obtained at the above-barrier energy of $E_{c.m.} = 144.0$ MeV agrees with the calculation within the error, which means that fusion is the main process after the system is captured inside the Coulomb barrier. The fragment mass distribution at this energy is Gaussian with mass symmetry, which is typical for compound nucleus fission. In the sub-barrier energy of $E_{c.m.} = 133.0$ MeV, the cross section for ^{264}Sg (4n) is a few factors smaller than the calculations, which shows that quasifission competes against fusion [12]. The quasifission fragment should be included in the fragment mass distribution. From the different structure of mass distribution between $E_{c.m.} = 144.0$ and 134.0 MeV, we conclude that the mass-asymmetric channel at $A_L/A_H \approx 90/178$ originates from quasifission. The yield for the asymmetric fission relative to that for the symmetric fission increases at $E_{c.m.} = 129.0$ MeV, close to the incident energy of 128.0 MeV at which the upper-limit cross section for ER is given. This indicates the quasifission probability increases.

In the $^{36}\text{S} + ^{238}\text{U}$ reaction [11] we observed a transition from symmetry to asymmetry mass distributions when the beam energies were decreased from the above-barrier to sub-barrier values. The phenomenon was interpreted by the effects of nuclear orientation on fusion and/or quasifission. At the sub-barrier energy, projectiles collide on the polar sides of the ^{238}U nucleus. In this case the reaction starts from the more distant contact point with a large charge-center distance, which results in a larger quasifission probability than the reactions starting from the equatorial collisions. This interpretation holds for the present observation in $^{30}\text{Si} + ^{238}\text{U}$.

The observed mass asymmetry in the quasifission for $^{30}\text{Si} + ^{238}\text{U}$ is different from those in heavier projectiles bombarded on actinide target nuclei. The quasifission in $^{36}\text{S} + ^{238}\text{U}$ has a mass asymmetry of $A_L/A_H \approx 74/200$ [11]. In the reactions of $^{48}\text{Ca} + ^{238}\text{U}$, ^{244}Pu , ^{248}Cm [7], the heavy fragment has a peak around $A_H \approx 210$. According to the mass asymmetry parameter $\alpha = (A_H - A_L)/(A_H + A_L)$, quasifission channels are located at $0.42 \sim 0.46$. The $^{30}\text{Si} + ^{238}\text{U}$ reaction has a significantly small α value of 0.33.

The potential energy landscape of ^{268}Sg felt by the system has the nearly similar structure to ^{274}Hs produced by $^{36}\text{S} + ^{238}\text{U}$ (see Fig. 4 in [11]) and has two distinct fission valleys. One is the symmetric fission channel ($\alpha = 0$), which is created by the larger binding energy of the fragments near the double-magic nucleus ^{132}Sn . The other is the asymmetric channel, which is connected to the shells around ^{78}Ni and ^{208}Pb ($\alpha = 0.4 \sim 0.5$). The α parameter of 0.33 observed in $^{30}\text{Si} + ^{238}\text{U}$ does not fit any minima of these valleys.

We made a model calculation to discuss the measured asymmetric fission channel at $\alpha = 0.33$. The Langevin equation was used to calculate a dynamical evolution of the nuclear shape from an initial contact point. The two-center shell model was used to calculate the potential energy of a nucleus whose shape is defined by z (charge center distance), δ (deformation), and α (mass asymmetry) [19]. The deformation of ^{238}U and the nuclear orientation at the initial contact was considered. The trajectories of the system

on the potential energy were calculated with a Monte Carlo method. Fusion is defined as the case when the trajectory enters inside the local energy minimum corresponding to the compound nucleus, whereas quasifission is defined as disintegration without reaching the minimum. The calculated mass distributions are shown in Fig. 4, where the spectrum is normalized such that the total cross section integrated over the mass is equal to those for the experimental mass distribution. The calculation reproduces the global distribution, especially the appearance of the asymmetric fission at the sub-barrier energy is reproduced. The fusion-fission spectra in the calculation are also shown in Fig. 4 (filled histogram). It is Gaussian with mass symmetry, and the standard deviation is almost constant with 21 u in the energies of $E_{c.m.} = 129.0\text{--}149.0$ MeV. The value is significantly smaller than $37\sim 38$ u determined from the measured distributions at the sub-barrier energies of 129.0 and 134.0 MeV (see Fig. 4). Furthermore the calculated fusion-fission does not show any asymmetric fission channels. The calculation supports that the observed asymmetric channel emerging at the sub-barrier energy is quasifission.

We also made the same calculation in the $^{36}\text{S} + ^{238}\text{U}$ reaction [11]. A good agreement with the measured mass distribution was obtained, and the mass asymmetric channel at $A_L/A_H = 74/200$ ($\alpha = 0.46$) was found to be quasifission [20].

In the $^{30}\text{Si} + ^{238}\text{U}$ reaction the trajectories approach the shape with smaller z but larger δ values before disintegrating as quasifission than the shape reached in the $^{36}\text{S} + ^{238}\text{U}$ reaction. The potential energy at this point felt by the former reaction shows that the fission channel leading to $^{208}\text{Pb}/^{78}\text{Ni}$ diminishes but a new fission channel with mass asymmetry $\alpha \sim 0.3$ opens instead. The quasifission follows this channel [20].

From the calculation shown in Fig. 4 we determined the fusion probability P_{fus} by the ratio of fusion-fission events to the total-fission events. The P_{fus} are 0.28 ($E_{c.m.} = 128.0$ MeV), 0.33 (133.0 MeV), and 0.41 (144.0 MeV), corresponding to the energies where the ER measurement was carried out. These values are larger than the fusion probabilities for the $^{34}\text{S} + ^{238}\text{U}$ reaction [21]. The calculated ER cross sections in Fig. 3(b) are multiplied by P_{fus} to estimate the cross sections correctly, and we obtained 8 (128.0 MeV), 11 (133.0 MeV), and 38 pb (144.0 MeV). The values agree with the measured ER cross sections.

The asymmetric fission channel was not clearly observed in the fragment mass distributions in the $^{16}\text{O} + ^{238}\text{U}$ reaction [22], although the standard deviation of the distributions increases in the sub-barrier energies. The reaction $^{26}\text{Mg} + ^{248}\text{Cm}$ also does not show asymmetric fission channel [7]. Silicon-30 is the lightest projectile among the measured reactions that the quasifission channel is observed.

The mass asymmetry of quasifission would contain information on how closely the system approaches the shape of compound nuclei. What would be interesting is to investigate the reaction using projectiles between magnesium and sulfur to understand the dynamic effects in heavy-ion reactions.

ACKNOWLEDGMENTS

The authors thank the crew of the JAEA tandem facility for the beam operation. We also thank Dr. Hagino of Tohoku University for fruitful discussions. This work was supported by a Grant-in-Aid for Scientific Research from the Japan Society for the Promotion of Science.

-
- [1] Yu. Ts. Oganessian, *J. Phys. G* **34**, R165 (2007).
 - [2] S. Hofmann and G. Münzenberg, *Rev. Mod. Phys.* **72**, 733 (2000).
 - [3] K. Morita *et al.*, *J. Phys. Soc. Jpn.* **73**, 1738 (2004).
 - [4] V. Zagrebaev and W. Greiner, *J. Phys. G* **31**, 825 (2005).
 - [5] W. Q. Shen *et al.*, *Phys. Rev. C* **36**, 115 (1987).
 - [6] J. Töke *et al.*, *Nucl. Phys. A* **440**, 327 (1985).
 - [7] M. G. Itkis *et al.*, *Nucl. Phys. A* **787**, 150c (2007).
 - [8] G. N. Knyazheva *et al.*, *Phys. Rev. C* **75**, 064602 (2007).
 - [9] A. Yu. Chizhov *et al.*, *Phys. Rev. C* **67**, 011603 (2003).
 - [10] R. N. Sagaidak *et al.*, *Phys. Rev. C* **68**, 014603 (2003).
 - [11] K. Nishio *et al.*, *Phys. Rev. C* **77**, 064607 (2008).
 - [12] K. Nishio *et al.*, *Eur. Phys. J. A* **29**, 281 (2006).
 - [13] R. Vandenbosch and J. R. Huizenga, *Nuclear Fission* (Academic Press, New York, 1973).
 - [14] Modified version of the CCFULL code, K. Hagino *et al.*, *Comput. Phys. Commun.* **123**, 143 (1999).
 - [15] K. Nishio *et al.*, *Phys. Rev. Lett.* **93**, 162701 (2004).
 - [16] R. H. Spear *et al.*, *At. Data Nucl. Data Tables* **42**, 55 (1989).
 - [17] S. Raman *et al.*, *At. Data Nucl. Data Tables* **36**, 1 (1987).
 - [18] W. Reisdorf and M. Schädel, *Z. Phys. A* **343**, 47 (1992).
 - [19] Calculation is based on the model in Y. Aritomo, *Phys. Rev. C* **80**, 064604 (2009), but effect of nuclear orientation was taken into account (in preparation).
 - [20] Y. Aritomo *et al.* (in preparation).
 - [21] K. Nishio *et al.*, *Phys. Rev. C* **82**, 024611 (2010).
 - [22] D. J. Hinde *et al.*, *Phys. Rev. C* **53**, 1290 (1996).